Dalton Transactions

Synthesis and electropolymerization of N-heterocyclic carbene complexes of Pd(II) and Pt(II) from an emissive imidazolium salt with a terthiophene backbone

Journal:	*Dalton Transactions*
Manuscript ID	DT-ART-08-2019-003363.R1
Article Type:	Paper
Date Submitted by the Author:	05-Sep-2019
Complete List of Authors:	Jones, Richard; University of Texas at Austin, Department of Chemistry Wang, Weiran; University of Texas at Austin, Department of Chemistry Guo, Hongyu; University of Texas at Austin, Department of Chemistry

ARTICLE

Synthesis and electropolymerization of N-heterocyclic carbene complexes of Pd(II) and Pt(II) from an emissive imidazolium salt with a terthiophene backbone.

Received 00th January 20xx,
Accepted 00th January 20xx

DOI: 10.1039/x0xx00000x

Weiran Wang, Hongyu Guo and Richard A Jones*

The synthesis of an emissive terthiophene-based imidazolium iodide: 1,3-dimethyl-4,6-di(thiophen-2-yl)-thienoimidazol-3-ium iodide (**4**), the corresponding *N*-heterocyclic carbene (NHC) proligand, and Pd and Pt-NHC complexes (**5a**, **5b**) are reported. A related Pd-NHC complex (**8**) with a mono-thiophene backbone has also been synthesized. The solid-state structures were determined by single crystal X-ray diffraction studies. Compounds **4**, **5a and 5b** were characterized by absorption/emission spectroscopy and an emission-quench phenomenon of **5a** was observed. The Pd complexes **5a** and **8** were shown to catalyze Heck type C-C bond forming reactions. The compounds with terthiophene backbones (**4**, **5a, 5b**) were electropolymerized onto indium tin oxide (ITO)-coated glass electrodes to yield thin films of conducting metallopolymers (CMPs) (**P1-3**). UV-vis-NIR spectroelectrochemistry data of **P1-3** showed reversible color changes upon oxidation due to the generation of charge carrier species along the polythiophene backbones.

Introduction

Polythiophene (PT) derivatives are π-conjugated organic polymers with narrow bandgaps (~2.0 eV), good environmental stabilities and mechanical flexibility which enables them to be used for the fabrication of organic electronic materials.[1] When properly functionalized with thiophene derivatives, metal complexes can be electropolymerized through the thiophene moieties with the metal center incorporated into the PT-based conducting polymer[2] thus generating new types of conducting metallopolymer (CMPs) based materials. The PT based CMPs have been used for various applications such as heterogeneous catalysis,[3] photoluminescent materials,[4] electrochromic glasses,[5] redox-active materials,[6] spin-crossover materials,[7] semiconductors[8] and small molecule sensors[9].

N-heterocyclic carbenes (NHCs) are known to be excellent σ-donor ligands in organometallic chemistry with rich chemical and structural versatility.[10] Two strategies have been used to incorporate NHC-metal complexes into PT-based CMPs via the synthesis of a modified NHC ligand with an electropolymerizable thiophene moiety.

Cowley and co-workers modified the ethylene backbone in an NHC with bithiophenes and synthesized the Ag (I), Au (I) and Ir (I) complexes as electropolymerizable monomers (Scheme 1a).[5c, 11] The CMPs containing Ag (I) and Ir (I) displayed electrochromic behaviors with color changes from yellow to dark blue when electrochemically oxidized from the neutral state.[5c] Song and co-workers functionalized the *N*-substituent in a NHC ligand with bithiophenes and synthesized its coinage metal complexes (Ag (I), Cu (I) and Au(I)) as electropolymerizable monomers (Scheme 1b).[5d] The synthesized CMPs of these complexes showed electrochromic behaviors with color changes from yellow/orange to dark yellow/green when electrochemically oxidized from the neutral state. In both strategies, the imidazole-2-ylidene is directly embedded into the conducting polymer backbone. To the best of our knowledge there have, so far, been no reports of a synthetic strategy in which the imidazole-2-ylidene and bound metal complex are tethered to the polythiophene

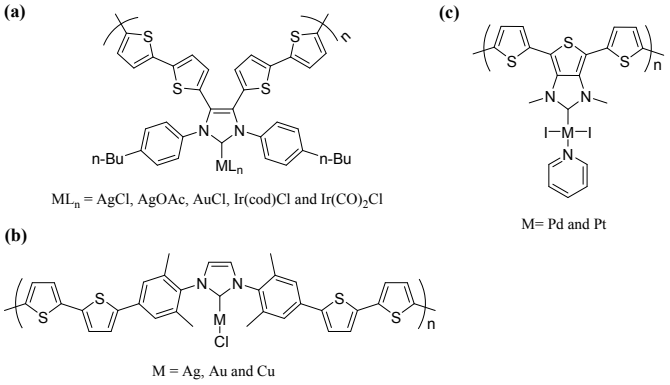

Scheme 1. Thiophene-based π-conjugated polymers incorporated NHC complexes: (a) Cowley and co-workers (refs 5c, 11). (b) Song and co-workers (ref 5d). (c) this work.

Department of Chemistry, The University of Texas at Austin, 105 E. 24th Street, Stop A5300, Austin, Texas 78712-1224, USA. E-mail: rajones@cm.utexas.edu

Electronic Supplementary Information (ESI) available: CV of compound **6** and P**1-3,** deconvoluted XPS spectra of **P1-3,** spectroscopic images for all new compounds (^{1}H NMR, ^{13}C NMR) and text tables of crystallographic data, DFT optimized coordinates. See DOI: 10.1039/x0xx00000x

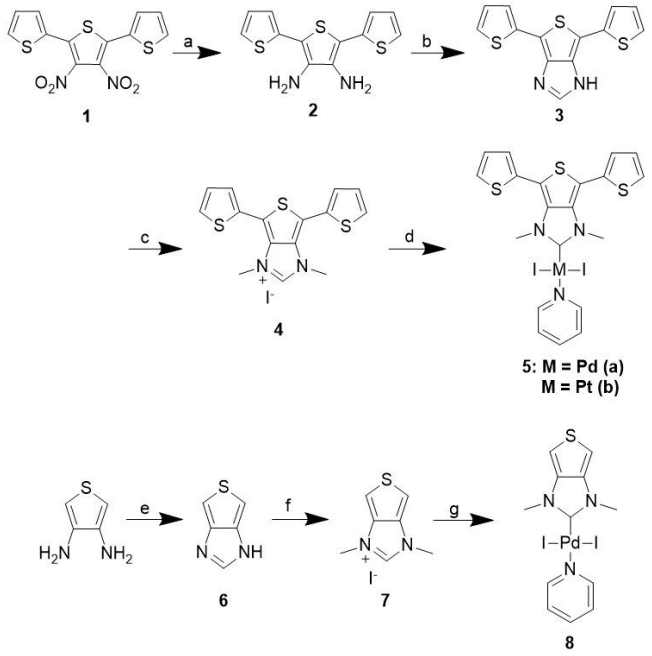

(a) Fe powder, AcOH, 65 °C, 30 min. (b). $HC(OMe)_3$, ACN, 90 °C, 16 h; (c) MeI; ACN; 100 °C, 40 h. (d) $PdCl_2(ACN)_2$ or $PtCl_2$, KI , K_2CO_3; pyridine; 80 °C, 12-40h. (e) $HC(OMe)_3$, ACN, 80 °C, 18 h. (f) MeI; ACN; 100 °C, 40 h. (g) $PdCl_2(ACN)_2$, KI , K_2CO_3 ; pyridine; 115 °C, 16 h.

Scheme 2. Synthesis of Pd-NHC (**5a**, **8**) and Pt-NHC (**5b**) complexes.

backbone through π-conjugation. We designed 1,3-dimethyl-4,6-di(thiophen-2-yl)-thienoimidazol-3-ium iodide (**4**) as a preligand, which can be synthesized from 3',4'-dinitro-2,2':5',2''-terthiophene (**1**)[12] in a 3-step strategy. Compound **4** can be further deprotonated and metallated to obtain metal-NHC complexes (Scheme 2). It is also known that terthiophene containing metal-salen complexes can be electropolymerized to provide CMPs.[8a, 9b, 13] We therefore expected that new metal-NHC complexes would also serve as electropolymerizable monomers for new CMPs (Scheme 1c). In these CMPs, the imidazole-2-ylidene moiety connects the PT backbone through π-conjugation. Since **4** is emissive, we were also interested in probing the photophysical properties of its corresponding NHC complexes. In order to compare the structural and electrochemical features of the new terthiophene-based NHC complexes, we also designed an NHC ligand with a mono-thiophene backbone and synthesized its Pd complex (**8**) (Scheme 2).

Herein we report the syntheses and structural characterizations of the new emissive terthiophene-based *N,N'*-dimethyl-imidazolium iodide (**4**) and a new *N,N'*-dimethyl-thienoimidazolium salt (**7**) as precursors for NHC ligands and corresponding Pd (**5a, 8**) and Pt (**5b**) complexes. The emissive properties of **4**, **5a** and **5b** were also investigated. In addition, we report the electrochemical synthesis and characterization of the conducting polymers **P1**, **P2** and **P3** obtained from **4**, **5a** and **5b**, respectively on indium tin oxide (ITO)-coated glass electrodes. The electrochromic properties of **P1-3** studied by UV-vis-NIR spectroelectrochemistry are also discussed.

Results and Discussion

Synthesis

Scheme 2 shows the overall synthetic route and details of reaction conditions for all new compounds. We firstly synthesized 4,6-di(thiophen-2-yl)-thienoimidazole (**3**) by cyclization of (2,2':5',2''-terthiophene)-3',4'-diamine (**2**) with $HC(OMe)_3$ in acetonitrile (ACN). Terthiophene-based *N,N'*-dimethyl-imidazolium iodide (**4**) was then obtained in good yield by reacting (**3**) with excess MeI in ACN at 100 °C for 40 hours. The analogous *N,N'*-dimethyl-imidazolium salt with a mono-thiophene backbone (**7**) was synthesized using a similar 3-step strategy from 3,4-diaminothiophene by cyclization with trimethyl orthoformate then methylation with excess MeI in ACN. Attempts to isolate the free carbene from **4** were unsuccessful. For example, 50 µmol of **4** in dry THF (3 mL) was deprotonated with 1 equiv. of lithium bis(trimethylsilyl)amide (LiHMDS, 50 uL of a 1.0 M solution in THF) and the mixture stirred at room temperature for 20 minutes, then the solvent was removed by vacuum. Upon addition of the LiHMDS solution, the yellow solution turned an intense dark red color. ^{1}H-NMR (600 MHz, C_6D_6) analysis of the resulting dark red solid indicated the formation of a complex mixture of products which could not be identified or isolated. This is probably due to the thermal instability of the free carbene of **4.** Previously reported 1,3-dimethylimidazol-2-ylidene[14] exhibits similar behavior involving thermal decomposition.

Despite the instability of the free carbene, metal-NHC complexes of **4** were prepared by the *in-situ* metalation of the imidazolium precursor. Thus **5a** and **5b** were prepared as pyridine adducts by heating **4** with the corresponding metal precursors in the presence of K_2CO_3 and KI in pyridine at 80-115 °C. NMR studies confirmed the formation of metal-carbene complexes by the diagnostic ^{13}C signal for the metal bound carbon which shifts from 155 ppm, in the imidazolium iodide, to 177 ppm (**5a**) and 165 ppm (**5b**). In a similar fashion, **8** was prepared by reacting $PdCl_2(ACN)_2$ with K_2CO_3 and KI in pyridine at 115 °C with a diagnostic Pd bound carbene ^{13}C NMR signal at δ = 174.99 ppm in $CDCl_3$ solution.

X-ray crystal structures

Fig. 1 shows views of the molecular structures of **4, 5a-b** and **8** from single-crystal X-ray diffraction studies. The imidazolium salt **4** crystalized in the $P\bar{1}$ space group with similar bond lengths for N1-C14 and N2-C14 (1.328 and 1.329 Å respectively) with a N1-C14-N2 bond angle of 112.78°. These structural features can be compared to those of the previously reported *N,N'*-dimethyl-benzimidazolium iodide (1.320 Å C-N and 110.65° C-N-C).[15] The slightly longer bonds and wider C-N-C bond angle indicate weaker conjugation of the thienyl imidazolium moiety compared to the corresponding benzimidazolium salt. The complexes **5a** and **5b** are

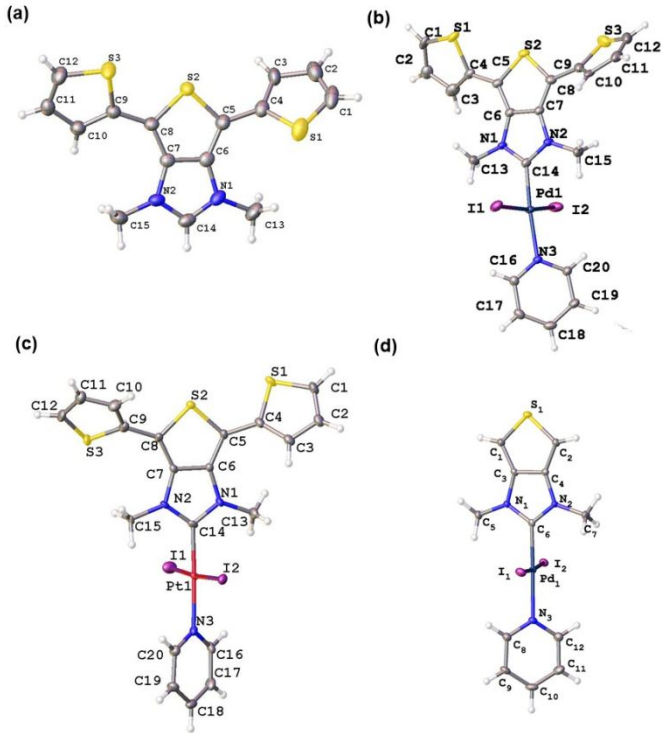

Fig. 1. View of the imidazolium cation in **4** (a), **5a** (b), **5b** (c) and **8** (d) showing the atom labeling schemes. Displacement ellipsoids are scaled to the 50% probability level. The minor components of the disordered thiophene in the terthiophene moiety were omitted for clarity.

isostructural and crystallize in the monoclinic space group *P2₁/c* with two trans-iodides coordinated to the square planar Pd or Pt metal centers. Compared to the imidazolium precursor, both N1-C14 and N2-C14 are elongated due to the loss of π-delocalization (for **5a**, 1.363 and 1.349 Å; for **5b**, 1.352 and 1.358 Å) and they both have a narrower N1-C14-N2 bond angle (108.83° **5a**, 108.09° **5b**). Both **5a** and **5b** have nearly the same metal-carbene bond length (Pd-C14: 1.958 Å and Pt-C14 1.946 Å, respectively), and similar metal-pyridine distances (Pd-N3: 2.077 Å and Pt-N3: 2.112 Å). The monothiophene based complex **8** co-crystallized in *P2₁/c* with 1 equiv. of CH_2Cl_2 in the asymmetric unit and two *trans*-iodides coordinated to the square planar Pd metal center (Pd-C bond length: 1.953 Å; Pd-N bond length: 2.102). The NHC moiety of **8** has an N-C-N angle of 108.49° and two C-N bonds of 1.352 Å and 1.353 Å with the Pd-C6 bond length = 1.962 Å and Pd-N3 bond length = 2.102 Å. All these structural features are similar to those of the terthiophene analog **5a**.

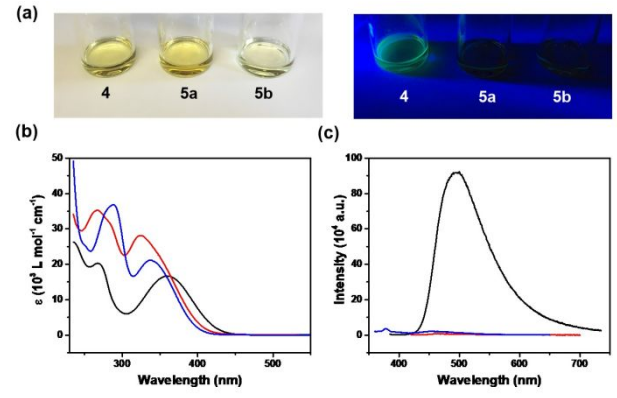

Fig. 2. a) CH_2Cl_2 solutions of **4** (3.7 mM), **5a** (3.6 mM) and **5b** (3.6 mM) in daylight (left) and 395 nm UV (right). (b) Stacked molar absorptivity traces of **4** (black line), **5a** (red line) and **5b** (blue line) in CH_2Cl_2. (c) Stacked emission traces of **4** (3.1 μM, CH_2Cl_2, black line), **5a** (3.4 μM, CH_2Cl_2, red line) and **5b** (3.4 μM, CH_2Cl_2, blue line).

Emission Properties

The imidazolium salt **4** and the carbene complexes **5a** and **5b** are pale yellow in solution under ambient light. When illuminated at 395 nm (UV handlamp) only **4** is emissive in the visible region. The absorption and emission spectra for **4, 5a** and **5b** in CH_2Cl_2 are also shown in Fig. 2.

The imidazolium salt **4** is emissive with absorption bands at 269 nm and 360 nm (Fig. 2b black) and an emission band at 495 nm in CH_2Cl_2 (Fig. 2c). Carbene complexes **5a** and **5b** have a similar level of molar absorptivity with two absorption bands (**5a**: 268 and 325 nm; **5b**: 288 and 340 nm) (Fig. 2b). Coordination of the carbene to the metal centers with pendant pyridine ligands effectively quenches the ligand-based emission. Thus, the emission intensities of **5a** and **5b** were negligible at the same concentration as **4** (Fig. 2c).

To further understand the effect of the carbene-bound metal center on the electronic structure of **4** and to investigate the photophysical changes between **4** and **5a**, Density Functional Theory (DFT) calculations were performed to determine the frontier orbital spatial distributions of electron density, using the atomic coordinates from the crystal structures of **4** and **5a** in a single point calculation. Fig. S1 shows the HOMO/LUMO of **4** and **5a**. For compound **4** the HOMO and LUMO overlap spatially. The HOMO is centered on the terthiophene moiety and the N atoms of the imidazolium while the LUMO is centered across the entire molecule. For **5a**, the HOMO is centered on the Pd center and pendant iodides and the LUMO is centered on the ligand. In this case there is no spatial overlap between HOMO and LUMO leading to no effective energy transfer and thus the corresponding first excited singlet state (S_1) for **5a** is a not emissive.

Catalytical Activity Studies.

Since NHC-Pd complexes have been reported to be powerful catalysts for various Pd-catalyzed cross-coupling reactions,[16] we also tested the catalytic activity of the new NHC-Pd complexes **5a** and **8**. The attempted Suzuki reaction (Scheme 3a), in the presence of **5a** or **8,** failed to give any conversion toward the target product. This result may be due to the small steric hindrance from the *N*-substituted methyl group, since steric bulk in NHCs are crucial to the reductive elimination step.[16a] However, both **5a** and **8** catalyzed the Heck reaction (Scheme 3b) with a high isolated yield of the

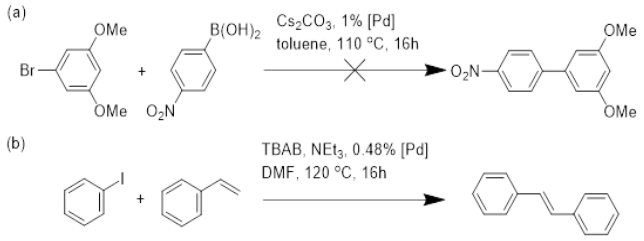

Scheme 3. Tested Pd catalyzed cross-coupling reactions ([Pd] = **5a** or **8**).

target compound (79% and 84% for **5a** and **8**, respectively) at a very low catalyst loading (0.48%). This is consistent with a previously reported NHC-Pd complex that catalyzed the Heck reaction. In this case NHC stabilized Pd(0) clusters, generated during the catalytic cycle in presence of NEt_3 and tetra(*n*-butyl)ammonium bromide (TBAB), catalyzed the Heck reaction with high catalytic activity.[17] This may also be the case for **8** although we have not performed any experiments designed to investigate this possibility.

Electropolymerization & Electrochemistry.

Conducting metallopolymers (CMPs) **P1**, **P2** and **P3** were synthesized from **4**, **5a** and **5b**, respectively, by oxidative electropolymeriztion of the corresponding monomer in CH_2Cl_2 solution with 0.1 M tetra(n-butyl)ammonium hexafluorophosphate ($TBAPF_6$) as supporting electrolyte. All CMPs were directly synthesized as thin films coated onto the surface of a working ITO-coated glass electrode using cyclic voltammetry (CV). **P1** is a burgundy colored film while **P2** and **P3** are both orange.

Fig. 3 shows the CV traces of **4**, **5a-b** and **8**. The CV of **4** (Fig. 3a) revealed two quasi-reversible electron transfers at $E_{1/2}$ = 0.16 V and 0.38 V and one irreversible terthiophene-based electron transfer at $E_{ox.}$ = 1.13V for the first scan. The amount of deposited polymer increases linearly with increasing scan number (Fig. 3 insets). Due to the large excess of hexafluorophosphate anion (PF_6^-) compared to the monomer, an anion exchange from iodide to PF_6^- during the electropolymerization process is expected. The CV of **5a** (Fig. 3b) and **5b** (Fig. 3c) both revealed one oxidative irreversible electron transfer (0.90 V and 0.97 V for **5a** and **5b**, respectively) and two irreversible reductive electron transfers (-0.64 V and 0.10 V for **5a** and -0.43 V and 0.16 V for **5b**) for the first scan. The polythiophene-based response was observed at $E_{ox.}$ = 0.60 V and 0.59 V, for **5a** and **5b** respectively starting with the 2nd scan. In order to further evaluate the electronic nature of the terthiophene moiety, the CV of **8** was also studied in CH_2Cl_2 or acetonitrile electrolyte solutions. We were unable to electropolymerize **8** in both electrolyte solutions using either ITO-coated glass or Pt working electrodes. Fig. S2 shows the representative CV of **8** in CH_2Cl_2 electrolyte solution. **8** shows a weak reversible electron transfer at $E_{1/2}$ = 1.42 V, two oxidative irreversible electron transfers at 1.00 V and 1.15 V and two reductive electron transfers at -0.92 V and -0.19 V, with a much smaller peak current (10 µA) compared to that of the terthiophene-based **5a** (281 µA, first scan). This data indicates that the elongation of the π system with additional thiophenes increases the electrical conductivity of the molecule, lowers the overall oxidation potential of the thiophene moiety and allows for the oxidative electropolymerization of the complexes featuring terthiophene moieties. Freshly synthesized **P1-3** were characterized by CV in monomer-free electrolyte solutions (CH_2Cl_2) under different scan rates from 50 mV/s to 250 mV/s

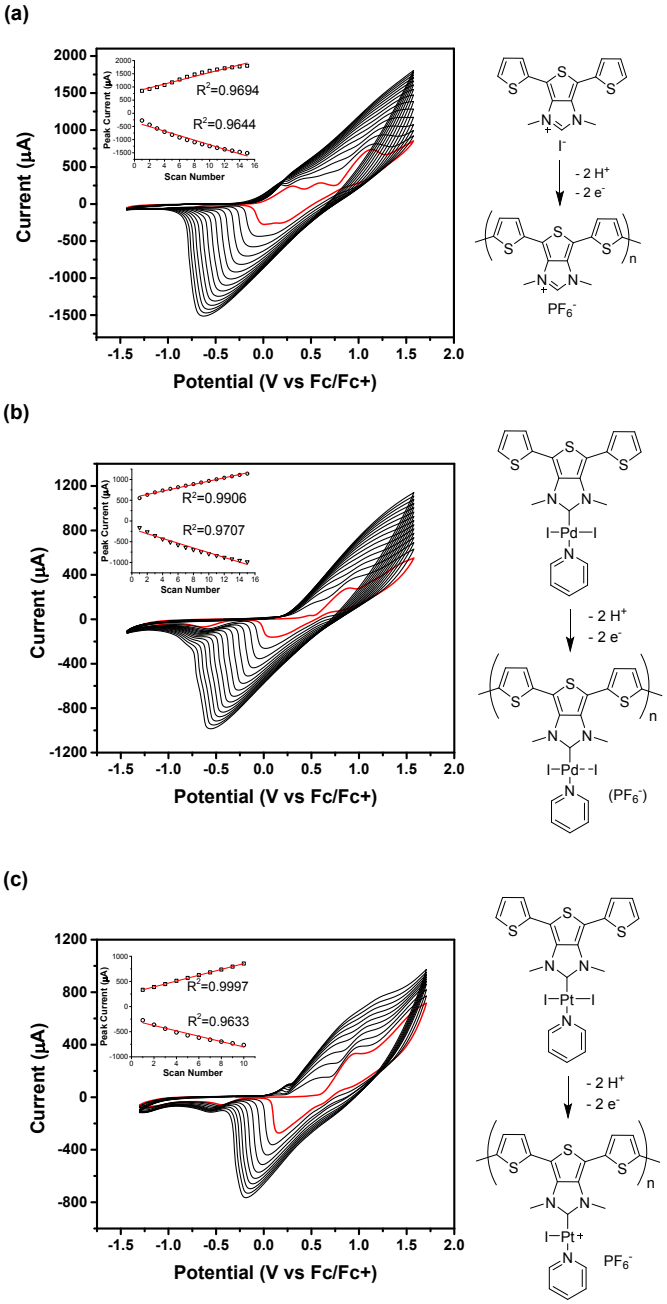

Fig. 3. Electropolymerization of imidazolium **4** in CH_2Cl_2 using a 0.8 mM monomer solution (a), complex **5a** in CH_2Cl_2 using a 0.7 mM monomer solution (b) and **5b** in CH_2Cl_2 using a 0.6 mM monomer solution (c). Insets show the linear relationship between current at peak oxidation/reduction potentials and number of scans.

(Fig. S3). All the thin films synthesized exhibited good stability in CH_2Cl_2. The linear relationship of observed oxidation/reduction peak current with scan rate in the range of 50 mV/s to 250 mV/s shows that **P1-3** are highly electroactive polymer thin films with porosities that did not limit the diffusion of electrolyte ions (Fig. S3 inset).

The CMPs **P1-3** on ITO-coated glass surfaces were also characterized by quantitative X-ray photoelectron spectroscopy (XPS) analysis. The XPS spectra of **P1, P2** and **P3** for specific elements are provided in the SI (Figs. S4, S5 and S6 respectively). **P1** was found to have an atomic ratio of S: P: F = 3.0: 1.0: 7.1 which is consistent with the predicted stoichiometric ratio of 3:1:6. **P2** was found to have an atomic ratio of Pd: S: I: P = 1.0: 2.9: 0.55 :1.2 and a precise P to F ratio of 1: 6.0 indicating the thin film contains hexafluorophosphate anions (PF_6^-). The S to Pd ratio confirmed the electropolymerization of **5a** through the terthiophene moiety. The two anions, PF_6^- and I^-, collectively give a ratio with respect to Pd (II) of 1.75 to 1. This reveals that an anion exchange reaction occurs during the electropolymerization under high electrolyte concentrations, with about 30% iodine dissociated and exchanged with PF_6^-. This then suggests that approximately 62% of the Pd complex in **P2** exists in the cationic form. **P3** shows an atomic ratio of Pt: S: I: P = 1.0: 2.9: 0.89 :0.96 and a P to F ratio of 1.0: 5.3. Thus, like **P2**, the S to Pt ratio shows that the polymer is formed via the electropolymerization of the terthiophene moiety. Note also that the Pt to I^- to PF_6^- ratio is nearly to 1:1:1, indicating that approximately one of two iodides bound to the Pt center is exchanged with PF_6^- during the electropolymerization. Again, this suggests that virtually all of the Pt-NHC complex exists in cationic form in the polymer.

Electrochromic properties

The polymer thin films **P1-3** on ITO-coated glass were further characterized by UV-vis-NIR spectroelectrochemistry. All the new metallopolymer thin films showed reversible electrochromic behavior driven by the generation of charge carrier species at the applied potentials. The color changes and spectroelectrochemical profiles of organic polymer **P1** and metallopolymer **P2** and **P3** resembled those of previously reported polythiophene polymers[18] and thiophene-based metal-NHC metallopolymers[5c, 5d]. Fig. 4 summarizes the absorption spectra of **P1-3** at different applied voltages. The neutral **P1** film is a dark red burgundy color with an absorption of π-π* transitions at 501 nm. Upon partial oxidation, the intensity at 501 nm decreases with bands at 845 nm and >1600 nm increasing in intensity. These are assigned to polaron formation along the backbone of the polymer. Once fully oxidized, **P1** is a pale blue color, the neutral π-π* transition is depleted and the two polaron bands merge into a single broad band at 1050 nm. This broad band is assigned to the bipolaron formed by further removal of electrons from the partially oxidized polymer backbone, resulting in the conversion of polarons to bipolarons. A similar trend was observed for **P2**. The neutral orange colored **P2** film absorbed at 420 nm. Its polaron bands grew in at 764 nm and 1405 nm when partially oxidized. Fully oxidized **P2** is a dark blue color with the neutral-state absorption depleted and a broad bipolaron absorption at 1035 nm tailing from the red visible absorption region (620~750 nm) to >1600 nm. The long absorption in the NIR region can be attributed to the generation of free charge carrier species leading to the metallic state of the polymer. **P3** is also orange with a neutral-state absorption band at 446 nm which decreases in intensity upon oxidization. When partially oxidized, bands at 880 nm and 1470 nm increase in intensity. The 878 nm band disappears when fully oxidized with the 1470 nm band gaining

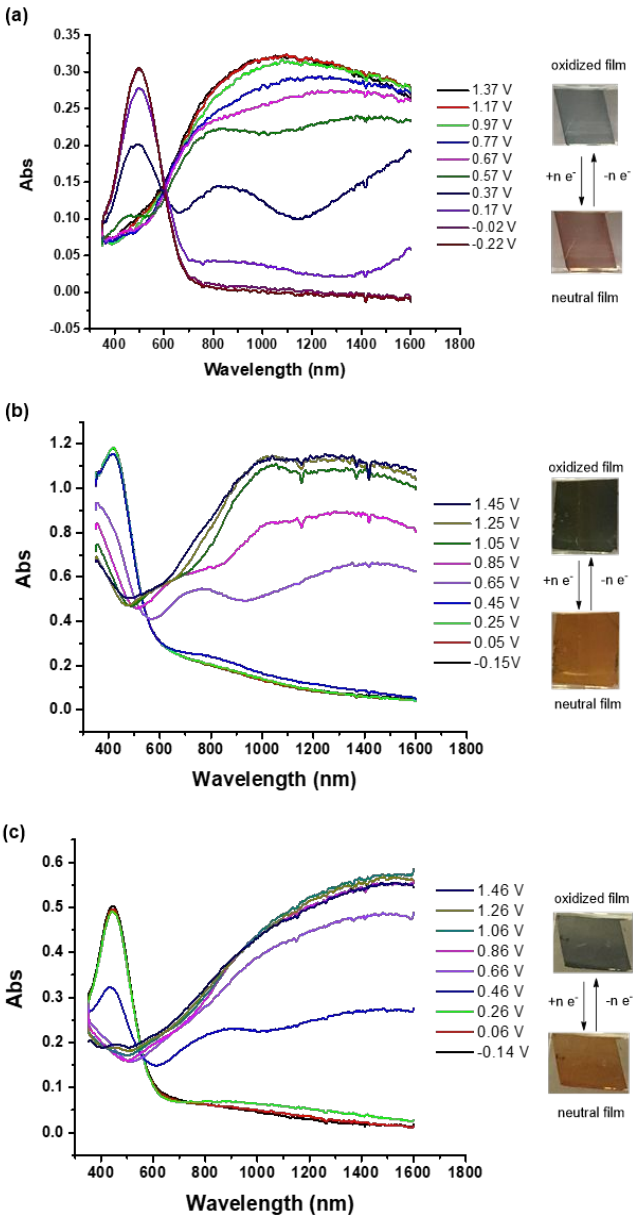

Fig. 4. UV-vis-NIR spectroelectrochemical spectra on ITO-coated glass substrates at different applied penitential vs. Fc/Fc^+ in CH_2Cl_2 electrolyte solution for **P1**(a), **P2**(b) and **P3**(c). All potentials are reported with referenced to Fc/Fc^+ couple as 0 V.

intensity. Here, the 880 nm band is assigned to the polaron absorption and 1470 nm to the bipolaron formation. Both polaron and bipolaron bands emerge when **P3** was partially oxidized, and the polaron transition disappeared when **P3** was fully oxidized. This is attributed to delocalization of electron density on the cationic Pt center leading to a much easier bipoloron formation. Fully oxidized **P3** is also dark blue due to the bipolaron absorption band tailing into the red visible absorption region. Note also that **P2** is harder to oxidize than **P1** and **P3** with an emerging polaron state at 0.55 V vs Fc/Fc^+ compared to **P1** (0.37 V vs Fc/Fc^+) and **P3** (0.46 V vs Fc/Fc^+) and fully oxidized at higher potential (1.05 V vs Fc/Fc^+) compared to **P1** (0.67 V vs Fc/Fc^+) and **P3** (0.77 V vs Fc/Fc^+). Incorporation of the metal center through carbene bonding does not alter the electronic properties of both monomer and synthesized polymer. We also tested the electrochromic reversibility of **P1-3** by running CV studies of each polymer thin film on ITO-coated glass electrodes as the working electrodes in CH_2Cl_2 electrolyte solutions. All polymer thin films showed excellent stability and the reversible color change was still observed after 100 CV cycles.

Conclusions

Imidazolium salts bearing terthiophene and mono-thiophene backbones were synthesized as precursors for new NHC ligands. The corresponding Pd and Pt complexes were also synthesized, and their molecular structures were determined by single-crystal X-ray diffraction studies. The terthiophene-based imidazolium salt and corresponding NHC complexes can be electropolymerized as thin films onto ITO-coated glass surfaces. The synthesized CMP thin films exhibit reversible electrochromic behavior from the generation of charge carrier species upon oxidation. To the best of our knowledge, this is the first report where Pt-NHC and Pd-NHC complexes have been incorporated into polythiophene based CMPs and the first reported example of 1,3-dimethyl-thienoimidazol-2-ylidene serving as an NHC ligand. Future studies in our group will focus on synthesizing metal complexes as electropolymerizable monomers using new NHC ligands and exploring their novel electronic properties.

Experimental procedures

General methods

Air- and moisture-sensitive reactions were carried out using either standard Schlenk techniques or in a dry box under an N_2 atmosphere. Acetonitrile, dimethylformamide (DMF) and CH_2Cl_2 used in air-sensitive reactions and all electrochemical experiments were dried via a two-column alumina purification system (Pure Process Technology, NH) and then degassed by purging under N_2 for 1h before storage over activated 3Å molecular sieves. Trimethyl orthoformate was dried by treatment with anhydrous $MgSO_4$ overnight and degassed with an N_2 purge for 1 hour before storage under N_2. Pyridine was distilled and stored over activated 3Å molecular sieves under N_2. Styrene was purified by passed through a short basic alumina column and then used immediately. Tetrabutylammonium hexafluorophosphate ($TBAPF_6$) was purchased from Oakwood and purified by triplicate recrystallizations from hot ethanol before drying under dynamic vacuum for three days. ITO-coated glasses (Rs = 70–100 Ω, 7 × 50 × 0.7 mm) were purchased from Delta Technologies, LTD and were cleaned by sonicating sequentially in acetone and CH_2Cl_2 prior to use. All other chemicals were purchased from commercial sources and used without further purification.

Characterization

^1H NMR spectra were recorded using either an Agilent 400 MR NMR spectrometer at 400 MHz, or a Bruker AVANCE III 500 MHz NMR at 500 MHz. Coupling constants are reported in hertz (Hz), and chemical shifts are reported in parts per million (ppm) relative to residual solvent peaks (residual $CDCl_3$ δH = 7.26 ppm, residual $(CD_3)_2SO$ δH = 2.50 ppm and residual CD_2Cl_2 δH = 5.32)[19] or tetramethylsilane (δH = 0.0). ^{13}C NMR spectra were recorded using a Bruker AVANCE III 500 MHz NMR at 125 MHz. Chemical shifts are reported as parts per million (ppm) relative to residual solvent peaks (residual $CDCl_3$ δC = 77.16 ppm, residual $(CD_3)_2SO$ δC = 2.50 ppm and residual CD_2Cl_2 δC = 53.84)[19] or tetramethylsilane (δC = 0.0). High-resolution mass spectra (HR-MS) were obtained on an Agilent Technologies 6530 Accurate Mass Q-TOF LC/MS instrument. Infrared spectra were recorded with either a Nicolet IR 200 FTIR spectrometer or a Bruker ALPHA II's Platinum ATR spectrophotometer. X-ray photoelectron spectra (XPS) were collected on a Kratos X-ray Photoelectron Spectrometer with a monochromatic Al Kα source (1486.7 eV). Pass energies of 20 and 80 eV were applied for high-resolution region spectra of different elements and survey spectra, respectively. The binding energies of **P1-3** were referenced to the sp^2 C 1s binding energy at 284.5 eV. Melting points were recorded with an OptiMelt Automated Melting Point System with digital image processing technology from Stanford Research System (SRS, Sunnyvale, CA) and the uncorrected values are reported.

Electrochemistry

Electrochemical studies were performed in a dry box under an N_2 atmosphere using GPES software from Eco. Chemie B. V. and an Autolab Potentiostat (PGSTAT30). All electrochemical experiments were performed with 0.1 M tetrabutylammonium hexafluorophosphate ($TBAPF_6$) as supporting electrolyte. All cyclic voltammetry experiments were carried out with an ITO-coated glass as the working electrode, a Pt wire coil counter electrode and an $Ag/AgNO_3$ reference electrode (silver wire dipped in a 0.01 M silver nitrate solution with 0.1 M $TBAPF_6$ in dry acetonitrile). All potentials were reported relative to the ferrocene/ferrocenium couple (Fc/Fc^+), which was used as an external standard to calibrate the reference electrode.

Spectroelectrochemistry

The *in-situ* UV-vis–NIR absorption-based spectro-electrochemical measurements were performed using the above described cell arrangement with a polymer film electrochemically deposited on ITO-coated glass substrate as the working electrode, a platinum wire as the counter electrode, and an $Ag/AgNO_3$ reference electrode. Experiments were carried out in an optical cuvette inside a dry box under an N_2 atmosphere. Absorption spectra were recorded on a Varian Cary 6000i UV-vis-NIR spectrophotometer within the NIR/vis spectral region ($1600 \geq \lambda \geq 350$ nm) under several applied potentials.

DFT calculations.

Theoretical calculations were carried out for compounds **4** and **5a** using density functional theory (DFT) as implemented in the Gaussian 09[20] package. Geometry optimizations and energy level calculations employed uB3LYP functional with 6-311G(d,p) basis set for compound **4**, and hybrid-DFT uB3LYP functional with SDD basis set for main group atoms and Lanl2dz pseudopotential basis set 8 for Pd for compound **5a**. All geometries were fully optimized using the default optimization criteria of the program. Orbital analyses were completed with the GaussView 5.0.9 program.

Single Crystal X-ray Diffraction

Suitable crystals were selected, covered with hydrocarbon oil and mounted on the tip of a nylon fiber on either a Rigaku AFC-12 diffractometer with a Saturn 724 CCD detector and a Rigaku XStream low temperature device (**4**, **5a**), or a Nonius Kappa CCD diffractometer with a Bruker AXS Apex II detector and an Oxford Cryosystems 700 low-temperature device (**5b**, **8**). Both diffractometers used a graphite monochromator with MoKα (λ = 0.71075). Crystals were kept at 100 K during the data collection process. Details of crystal data, data collection and structure refinement are listed in Table S1. Using Olex2[21], the structures were solved with the ShelXT[22] structure solution program using Intrinsic Phasing and refined with the ShelXL[23] refinement package using Least Squares minimization. CCDC 1947229-1947232

Synthesis

2, ([2,2':5',2''-terthiophene]-3',4'-diamine): To a 500 mL round bottom flask with a magnetic stir bar, **1**[24] (3.00 g, 8.90 mmol) and iron powder (250 mesh, 5.00 g, 89.6 mmol, 10 equiv.) were suspended in acetic acid (180 mL). The mixture was then stirred at 65 °C for 30 min under nitrogen before cooling to room temperature. The mixture was poured onto ice (500 g) and extracted with Et_2O (300 mL). The organic phase was shaken with several NaOH pellets to remove any remaining acetic acid. The mixture was further washed with saturated $NaHCO_3$ aqueous solution slowly until the solution turned basic, then washed with saturated brine before being collected and dried over $MgSO_4$. Solvent was removed by rotary evaporation to give the target compound a dark yellow solid. Yield: 2.29 g, 93%: The product was used directly without further purification.

3, (4,6-di(thiophen-2-yl)-1*H*-thieno[3,4-d]imidazole, **DTTI**): **2** (2.29 g 8.23 mmol) was dissolved in degassed ACN (100 mL) and $HC(OMe)_3$ (5.00 mL, 45.7 mmol, 5.5 equiv.) in a 250 mL Schlenk flask equipped with a magnetic stir bar and a condenser. The mixture was then refluxed at 90 °C for 24 h under N_2, before cooling to room temperature. The mixture was concentrated by rotary evaporation to 5 mL and dissolved in EtOAc (150 mL). The organic phase was washed with saturated $NaHCO_3$ aqueous solution followed by saturated brine. It was then dried over $MgSO_4$ and solvent removed by rotary evaporation to give dark yellow solid. The mixture was further purified on a silica gel column by elution with hexane to pure CH_2Cl_2 then 10% MeOH in CH_2Cl_2 to give the title compound as a yellow solid. Yield, 1.79, 77.7%: ^{1}H-NMR (400 MHz, $(CD_3)_2SO$) δ 12.36 (s, 1H), 8.36 (s, 1H), 7.50 (t, J = 4.2 Hz, 2H), 7.42 (dd, J = 13.9, 3.7 Hz, 2H), 7.19 – 7.07 (m, 2H). ^{13}C NMR (125 MHz, $(CD_3)_2SO$) δ 152.97, 134.75, 128.29, 124.61, 123.32, 123.09. FT-IR (cm^{-1}): 3081 (br, w), 1790 (w), 1639 (m), 1536 (w), 1517 (m), 1500 (w), 1479 (m), 1442 (w), 1421 (w), 1373 (m), 1341 (w), 1286 (m), 1254 (w), 1238 (w), 1224 (m), 1179 (w), 1129 (m), 1089 (w), 1070 (w), 1039 (w), 978 (w), 938 (w), 904 (w), 850 (m), 822 (m), 811 (m), 745 (w), 697 (s), 682 (s), 630 (w), 614 (s), 583 (w), 572 (w), 534 (w), 514 (m), 494 (w), 463 (m). HR-MS (ESI+): $[M+H]^+$ $C_{13}H_9N_2S_3^+$, calcd. 288.9922; found 288.9933. m.p.: darkens at 97 °C, vigorous decomposition at 157-8 °C.

4 (1,3-dimethyl-4,6-di(thiophen-2-yl)-thienoimidazol-3-ium iodide,TThIMeHI): **3** (504 mg, 1.75 mmol 1 equiv.) and MeI (0.75 mL, 12 mmol, 5.7 equiv.) were suspended in acetonitrile (4 mL) in a 10 mL Chemglass heavy wall pressure vessel with a magnetic stir bar. The mixture was degassed by bubbling N_2 through the stirred mixture for 5 minutes then sealed with a cap and stirred at 100 °C for 40 hours in an oil bath. After cooling to room temperature, the mixture was diluted to 100 mL in volume with CH_2Cl_2 and washed with a cold saturated aqueous KI solution (2 x 50 mL). The solution was then dried over $MgSO_4$ and filtered. The solvent was removed under vacuum. The resulting dark mixture was heated under reflux in a mixture of CH_2Cl_2 (3 mL) and Et_2O (120 mL) before being cooled to -20 °C. The mixture was filtered and the solid washed with additional cold Et_2O (2 x 20 mL), followed by drying under vacuum. The product was obtained as a yellow solid. Yield, 600 mg, 77%: ^{1}H-NMR (500 MHz, $(CD_3)_2SO$) δ 9.69 (s, 1H), 7.86 (d, *J* = 5.1 Hz, 2H), 7.56 (d, *J* = 3.7 Hz, 2H), 7.27 (dd, *J* = 5.2, 3.6 Hz, 2H), 3.87 (s, 6H). ^{13}C-NMR (125 MHz, $(CD_3)_2SO$) δ 153.60, 131.65, 130.31, 129.89, 128.81, 128.25, 113.12, 35.46. HR-MS (ESI+): $(M-I)^+$, $C_{15}H_{13}N_2S_3^+$, calculated: 317.0235; found: 317.0233. FT-IR (cm^{-1}): 3153 (w), 3056 (m), 3002 (m), 2956 (m), 2827 (w), 1816 (w), 1578 (s), 1505 (w), 1477 (m), 1450 (s), 1386 (m), 1357 (m), 1315 (m), 1265 (w), 1217 (w), 1081 (s), 1043 (m), 955 (m), 913 (m), 875 (w), 833 (s), 723 (s), 701 (s), 593 (m), 569 (s), 534 (s), 503 (m), 479 (m), 426 (w). m.p.: 188-189 °C (dec.). Crystals suitable for single crystal X-ray

diffraction studies were grown by vapor diffusion of Et_2O into a concentrated solution of **4** in CH_2Cl_2 at -20 °C.

5a (Pd(TThIMe)(pyridine)I_2)**: 4** (112 mg, 0.25 mmol, 1 equiv.), $PdCl_2(acn)_2$ (65.7 mg, 0.25 mmol, 1 equiv.), KI (168 mg, 1.01 mmol, 4 equiv.) and K_2CO_3 (181 mg, 1.30 mmol, 5.2 equiv.) were added to an oven-dried 25 mL Schlenk flask equipped with a magnetic stir bar. The solid mixture was dried under vacuum for 1 hour and then dry pyridine (10 mL) was added. The mixture was stirred at 80 °C for 12 h before being allowed to cool to room temperature. The solvent was removed under vacuum and the residue dissolved in CH_2Cl_2 (5 mL). The solution was then filtered to remove precipitate. The solvent was removed under vacuum and the resulting solid was purified on a silica gel column with CH_2Cl_2 as the eluent. The product was obtained by recrystallization from CH_2Cl_2/Et_2O (1 mL/16mL) at -20 °C as a yellow crystalline solid. Yield, 74.7 mg, 40 %: ^{1}H-NMR (500 MHz, $CDCl_3$) δ 9.08 – 9.02 (m, 2H), 7.84 – 7.73 (m, 1H), 7.44 (dt, *J* = 5.2, 1.3 Hz, 2H), 7.40 – 7.32 (m, 2H), 7.20 (td, *J* = 3.7, 1.2 Hz, 2H), 7.12 (dd, *J* = 5.2, 3.6 Hz, 2H), 4.22 (s, 1H), 4.12 (s, 2H), 4.02 (s, 3H). ^{13}C NMR (125 MHz, $CDCl_3$) δ 177.36, 176.65, 153.87, 152.98, 151.15, 138.05, 137.82, 135.36, 135.30, 130.22, 130.13, 129.66, 129.61, 128.06, 127.99, 127.75, 124.68, 124.61, 108.12, 37.87, 37.57. FT-IR (cm^{-1}): 3085 (br, m), 2928 (br, w), 1602 (m), 1513 (w), 1444 (s), 1424 (m), 1407 (m), 1377 (s), 1352 (m), 1290 (w), 1231 (w), 1211 (w), 1176 (w), 1149 (w), 1100 (w), 1078 (m), 1068 (m), 1045 (m), 1016 (w), 999 (w), 956 (m), 946 (m), 931 (m), 832 (s), 766 (w), 751 (m), 723 (s), 701 (s), 687 (s), 657 (s), 641 (m), 631 (m), 576 (m), 540 (w), 530 (w), 504 (w), 482 (w). m.p.: 245 °C (dec.). Crystals suitable for single crystal X-ray diffraction studies were grown by layering pentane over a concentrated solution of **5a** in CH_2Cl_2 at -20 °C.

5b (Pt(TThIMe)(pyridine)I_2): **4** (112 mg, 0.25 mmol, 1 equiv.), $PtCl_2$ (72.0 mg, 0.27 mmol, 1.1 equiv.), KI (166.9 mg, 1 mmol, 4 equiv.) and K_2CO_3 (174.6 mg, 1.3 mmol, 5.2 equiv.) were added to a 50 mL oven-dried Schlenk flask equipped with a magnetic stir bar. The solid mixture was dried under vacuum for 1 hour before dry pyridine (10 mL) was added. The mixture was then stirred at 110 °C for 40 h before being allowed to cool to room temperature. The solvent was removed under vacuum and the residue dissolved in CH_2Cl_2 (10 mL). The solution was then filtered through a pad of silica gel and further eluted with additional CH_2Cl_2 (20 mL). The solvent was then removed under vacuum. The resulting solid was purified on a silica gel column with hexanes: CH_2Cl_2= 1:9 as the eluent to give the target compound as yellow solid. Yield, 71.8 mg, 34 %: ^{1}H NMR (500 MHz, CD_2Cl_2) δ 8.93 (d, *J* = 5.6 Hz, 2H), 7.72 (td, *J* = 7.6, 0.9 Hz, 1H), 7.40 (d, *J* = 5.1 Hz, 2H), 7.30 (t, *J* = 6.4 Hz, 2H), 7.19 – 7.13 (m, 2H), 7.03 – 7.09 (m, 2H), 3.93 (s, 6H). ^{13}C NMR (125 MHz, CD_2Cl_2) δ 165.48, 153.93, 138.31, 135.60, 130.89, 129.98, 128.30, 128.14, 125.48, 108.25, 37.34. HR-MS (ESI+): $(M+K)^+$, $C_{20}H_{17}I_2N_3PtS_3K^+$, calcd. :882.7948, found: 882.7954. FT-IR (cm^{-1}): 3085 (w), 3027 (w), 2923 (w), 2852 (w), 1739 (s), 1603 (m), 1555 (w), 1515 (w), 1505 (w), 1444 (s), 1423 (s), 1408 (s), 1376 (s), 1352 (s), 1289 (m), 1268 (m,br), 1231 (s), 1216 (s), 1208 (s), 1150 (w), 1102 (m), 1077 (m), 1069 (m), 1047 (m), 1018 (w), 998 (w), 958 (m), 933 (m), 831 (s), 755 (m), 722 (s), 703 (s), 680 (s), 648 (w), 634 (w), 578 (w), 542 (w), 531 (m), 503 (m), 483 (m), 447 (m), 425 (m), 408 (w). m.p.: 284 °C (dec.). Crystals suitable for single crystal X-ray diffraction studies were grown by vapor diffusion of Et_2O into a concentrated solution of **5b** in CH_2Cl_2 at -20 °C.

6 (1*H*-thieno[3,4-*d*]imidazole)**:** 3,4-diaminothiophene[24] (481.5 mg, 4.2 mmol, 1 equiv.) was dissolved in dry acetonitrile (15 mL) and trimethyl orthoformate (2.0 mL, 12 mmol, 2.8 equiv.) in an oven-dried 50 mL Schlenk flask equipped with a magnetic stir bar. The solution was then stirred at 80 °C overnight (18 h). After cooling to room temperature, the solvent was removed under vacuum. The residue was then dissolved in ethyl acetate (100 mL), and the solution filtered. The solution was then washed with saturated aqueous $NaHCO_3$ and saturated brine. After drying with $MgSO_4$, the solvent was removed under vacuum. The target compound was purified on a silica gel column with a gradient eluent from pure CH_2Cl_2 to 10% methanol in CH_2Cl_2 to give the title compound as a dark red solid. Yield, 371.9 mg, 71 %: ^{1}H NMR (400 MHz, $(CD_3)_2SO$) δ 11.62 (s, 1H), 8.21 (s, 1H), 7.01 (s, 2H). ^{13}C NMR (125 MHz, $(CD_3)_2SO$) δ 151.77, 144.95, 97.81. HR-MS (ESI+), $(M+H)^+$, $C_5H_5N_2S^+$, calcd. 125.0168, found: 125.0164. FT-IR (cm^{-1}): 3106 (w), 3060 (w), 2964 (w), 2917 (w), 2841 (w), 2800 (w), 2719 (w), 2575 (w), 1794 (w), 1661 (w), 1602 (m), 1553 (w), 1480 (s), 1450 (m), 1371 (s), 1277 (s), 1167 (m), 1134 (s), 1098 (m), 945 (s), 902 (m), 861 (w), 834 (w), 809 (s), 787(s), 749 (s), 730 (s), 640 (s), 603 (s), 520 (m), 449 (s).

7 (1,3-dimethyl-1*H*-thieno[3,4-*d*]imidazol-3-ium iodide, ThIMeHI)**: 6** (446 mg, 3.6 mmol, 1 equiv.) and $KHCO_3$ (377 mg, 3.8 mmol, 1.05 equiv.) were suspended in MeI (1.50 mL, 24 mmol, 6.7 equiv.) and acetonitrile (10 mL) in a 50 mL Chemglass heavy wall pressure flask equipped with a magnetic stir bar. The solution was degassed with a stream of N_2 for 5 min before being sealed. The mixture was stirred at 100 °C for 22 h before cooling to room temperature. The mixture was first filtered to remove KI and unreacted $KHCO_3$, then the solvent was removed by rotary evaporation. The resulting solid was suspended in acetone (20 mL) and supersonicated for 20 min. The mixture was then filtered and further washed with acetone twice (5 mL ea.) to give a pale yellow solid. Yield, 662.5 mg, 65.8%: ^{1}H NMR (500 MHz, $(CD_3)_2SO$) δ 9.57 (s, 1H), 7.82 (s, 2H), 3.90 (s, 6H). ^{13}C NMR (125 MHz, $(CD_3)_2SO$) δ 152.25, 136.44, 104.15, 34.77. HR-MS (ESI+): cation only (M^+, $C7H9N2S^+$), calcd.: 153.0481, found 153.0485. FT-IR (cm^{-1}): 3410 (br,w), 3108 (w), 3011 (w), 2929 (w), 1775 (w), 1755 (w), 1568 (s), 1557 (s), 1515 (m), 1453 (m), 1439 (m), 1417 (s), 1410 (s), 1396 (m), 1301 (s), 1292 (s), 1212 (w), 1199 (m), 1162 (m), 1142 (m), 1122 (m), 1092 (m), 1083 (m), 951 (m), 858 (m), 829 (w), 807 (s), 784 (s), 753 (s), 723 (m), 675 (m), 660 (w), 600 (m), 573 (s), 556 (s), 507 (w), 440 (s). m.p. 224 °C (dec.).

8 (Pd(ThIMe)(pyridine)I_2)**:** To a 25 mL oven-dried Schlenk tube with a magnetic stir bar was added **7** (112.3 mg, 0.40 mmol, 1 equiv.), $PdCl_2(acn)_2$ (102.8 mg, 0.396mmol, 0.99 equiv.), KI (267.4 mg, 1.61 mmol, 4 equiv.) and K_2CO_3 (278.8 mg, 2.02 mmol, 5 equiv.). The solid was dried under vacuum for 1 hour before being suspended in dry pyridine (10 mL). The mixture was then stirred at 80 °C for 16 h before being allowed

to cool to room temperature. The solvent was then removed under vacuum. The solid was dissolved in CH_2Cl_2 (30 mL) and the solution filtered through a pad of celite. The solution was then concentrated under vacuum to about 0.5 mL and purified on a silica gel column with CH_2Cl_2 as the eluent. The resulting reddish compound was recrystallized from CH_2Cl_2/Et_2O (5mL/ 20mL) at -20 °C to give an orange solid. Yield, 171.0 mg, 72.3%: ^{1}H-NMR (500 MHz, $CDCl_3$) δ 9.05 (s, 2H), 7.78 (ddd, J = 9.7, 6.5, 2.0 Hz, 1H), 7.37 (tt, J = 7.1, 3.4 Hz, 2H), 6.66 (s, 2H), 4.04 (s, 6H). ^{13}C NMR (125 MHz, $CDCl_3$) δ 174.99, 153.77, 139.87, 137.84, 124.59, 96.12, 36.91. m.p.: 219 °C (decomp.). FT-IR (cm^{-1}): 3094 (w), 2926 (w), 1736 (m), 1599 (m), 1520 (w), 1440 (s), 1417 (s), 1368 (s), 1256 (w), 1238 (w), 1214 (m), 1144 (s), 1095 (m), 1064 (s), 1041 (m), 1011 (m), 986 (w), 962 (m), 852 (w), 843 (m), 810 (s), 746 (s), 694 (s), 647 (s), 634 (s), 581 (s), 440 (m). Crystals suitable for single crystal X-ray diffraction studies were grown from vapor diffusion of Et_2O into a concentrated solution of **8** in CH_2Cl_2 at -20 °C.

Procedures for Heck reactions. In a 25 mL oven-dried Schlenk flask with a magnetic stir bar, iodobenzene (0.23 mL, 2.06 mmol, 1.0 equiv.), styrene (0.36 mL, 3.1 mmol, 1.5 equiv.), TBAB (645 mg, 2 mmol, 0.97 equiv.) and [Pd] (**5a**: 7.6 mg, **8**: 6.0 mg, 0.01 mmol, 0.48 %) were suspended in dry DMF (4 mL). Then triethylamine (0.56 mL, 4.02 mmol, 2.0 equiv.) was injected into the stirred solution. Then the flask was capped with a glass stopper and stirred at 120 °C for 16 h before being allowed to cool down to room temperature. The mixture was then poured over ice (50 g) and extracted with Et_2O (3 x 20 mL). The organic fractions were combined and washed with saturated NH_4Cl solution and saturated brine, before drying over $MgSO_4$. The solvent was then removed by rotary evaporation. The resulting off-white solid was purified on a silica gel column using 0.5% EtOAc in hexanes as the eluent, to give the title compound ((*E*)-stilbene) as a white solid. Yield, **5a**: 295 mg, 79.4%; **8**: 310 mg, 83.7%: ^{1}H NMR (500 MHz, $CDCl_3$) δ 7.51 (d, J = 7.3 Hz, 2H), 7.35 (t, J = 7.6 Hz, 2H), 7.25 (t, J = 7.4 Hz, 1H), 7.09 (s, 1H). ^{13}C NMR (125 MHz, $CDCl_3$) δ 137.32, 128.67, 127.61, 126.50. The spectroscopic data matches literature values.[25]

Conflicts of interest

There are no conflicts to declare

Acknowledgements

We thank Dr. Vincent M Lynch for help with X-ray diffraction and crystallographic studies. The purchase of the Bruker AVANCE III 500 spectrometer was made possible with NIH funding (1 S10 OD021508-01). We thank the Welch Foundation for support (F-816). We acknowledge the NSF (CHE-1807847) for support.

Notes and references

1. (a) Beaujuge, P. M.; Reynolds, J. R., *Chem. Rev.* **2010,** *110*, 268-320; (b) Roncali, J., *Chem. Rev.* **1997,** *97*, 173-206.
2. (a) Friebe, C.; Hager, M. D.; Winter, A.; Schubert, U. S., *Adv. Mater.* **2012,** *24*, 332-345; (b) Wolf, M. O., *Adv. Mater.* **2001,** *13*, 545-553.
3. (a) Albano, V. G.; Bandini, M.; Moorlag, C.; Piccinelli, F.; Pietrangelo, A.; Tommasi, S.; Umani-Ronchi, A.; Wolf, M. O., *Organometallics* **2007,** *26*, 4373-4375; (b) Bandini, M.; Pietrangelo, A.; Sinisi, R.; Umani-Ronchi, A.; Wolf, M. O., *Eur. J. Org. Chem.* **2009,** *2009*, 3554-3561; (c) Zulauf, A.; Mellah, M.; Guillot, R.; Schulz, E., *Eur. J. Org. Chem.* **2008,** *2008*, 2118-2129.
4. (a) Chen, X.-Y.; Yang, X.; Holliday, B. J., *J. Am. Chem. Soc.* **2008,** *130*, 1546-1547; (b) Keskin, S. G.; Zhu, X. J.; Yang, X. P.; Cowley, A. H.; Holliday, B. J., *Macromolecules* **2018,** *51*, 8217-8228; (c) Hesterberg, T. W.; Yang, X.; Holliday, B. J., *Polyhedron* **2010,** *29*, 110-115.
5. (a) Liang, Y.; Strohecker, D.; Lynch, V.; Holliday, B. J.; Jones, R. A., *ACS Appl. Mater. Interfaces* **2016,** *8*, 34568-34580; (b) Farrell, J. R.; Lavoie, D. P.; Pennell, R. T.; Cetin, A.; Shaw, J. L.; Ziegler, C. J., *Inorg. Chem.* **2007,** *46*, 6840-6842; (c) Powell, A. B.; Bielawski, C. W.; Cowley, A. H., *J. Am. Chem. Soc.* **2010,** *132*, 10184-10194; (d) Satheeshkumar, C.; Park, J.-Y.; Jeong, D.-C.; Song, S. G.; Lee, J.; Song, C., *RSC Adv.* **2015,** *5*, 60892-60897.
6. (a) Milum, K. M.; Kim, Y. N.; Holliday, B. J., *Chem. Mater.* **2010,** *22*, 2414-2416; (b) Wolf, M. O.; Wrighton, M. S., *Chem. Mater.* **1994,** *6*, 1526-1533.
7. (a) Djukic, B.; Seda, T.; Gorelsky, S. I.; Lough, A. J.; Lemaire, M. T., *Inorg. Chem.* **2011,** *50*, 7334-7343; (b) Djukic, B.; Lemaire, M. T., *Inorg. Chem.* **2009,** *48*, 10489-10491.
8. (a) Nguyen, M. T.; Jones, R. A.; Holliday, B. J., *Chem. Commun.* **2016,** *52*, 13112-13115; (b) Mejia, M. L.; Reeske, G.; Holliday, B. J., *Chem. Commun.* **2010,** *46*, 5355-5357.
9. (a) Holliday, B. J.; Stanford, T. B.; Swager, T. M., *Chem Mater* **2006,** *18*, 5649-5651; (b) Reddinger, J. L.; Reynolds, J. R., *Chem. Mater.* **1998,** *10*, 1236-1243.
10. (a) Hopkinson, M. N.; Richter, C.; Schedler, M.; Glorius, F., *Nature* **2014,** *510*, 485-496; (b) Poyatos, M.; Mata, J. A.; Peris, E., *Chem. Rev.* **2009,** *109*, 3677-3707.
11. Powell, A. B.; Bielawski, C. W.; Cowley, A. H., *J. Am. Chem. Soc.* **2009,** *131*, 18232-18233.
12. (a) Schwiderski, R. L.; Rasmussen, S. C., *J. Org. Chem.* **2013,** *78*, 5453-5462; (b) Wang, Z.; Gao, Z.; Feng, Y.; Liu, Y.; Yang, B.; Liu, D.; Lv, Y.; Lu, P.; Ma, Y., *Polymer* **2013,** *54*, 6191-6199.
13. (a) Reddinger, J. L.; Reynolds, J. R., *Macromolecules* **1997,** *30*, 673-675; (b) Reddinger, J. L.; Reynolds, J. R., *Chem. Mater.* **1998,** *10*, 3-5.
14. Arduengo, A. J.; Dias, H. V. R.; Harlow, R. L.; Kline, M., *J. Am. Chem. Soc.* **1992,** *114*, 5530-5534.
15. Huynh, H. V.; Ho, J. H. H.; Neo, T. C.; Koh, L. L., *J. Organomet. Chem.* **2005,** *690*, 3854-3860.
16. (a) Kantchev, E. A.; O'Brien, C. J.; Organ, M. G., *Angew. Chem. Int. Ed.* **2007,** *46*, 2768-2813; (b) Fortman, G. C.; Nolan, S. P., *Chem. Soc. Rev.* **2011,** *40*, 5151-5169.
17. Astakhov, A. V.; Khazipov, O. V.; Chernenko, A. Y.; Pasyukov, D. V.; Kashin, A. S.; Gordeev, E. G.; Khrustalev, V. N.; Chernyshev, V. M.; Ananikov, V. P., *Organometallics* **2017,** *36*, 1981-1992.
18. (a) Mastragostino, M.; Arbizzani, C.; Bongini, A.; Barbarella, G.; Zambianchi, M., *Electrochim. Acta* **1993,** *38*, 135-140; (b) Arbizzani, C.; Bongini, A.; Mastragostino, M.; Zanelli, A.; Barbarella, G.; Zambianchi, M., *Adv. Mater.* **1995,** *7*, 571-574.

19. Fulmer, G. R.; Miller, A. J. M.; Sherden, N. H.; Gottlieb, H. E.; Nudelman, A.; Stoltz, B. M.; Bercaw, J. E.; Goldberg, K. I., *Organometallics* **2010,** *29*, 2176-2179.
20. Gaussian 09, Revision D.01, Frisch, M. J.; Trucks, G. W.; Schlegel, H. B.; Scuseria, G. E.; Robb, M. A.; Cheeseman, J. R.; Scalmani, G.; Barone, V.; Mennucci, B.; Petersson, G. A.; Nakatsuji, H.; Caricato, M.; Li, X.; Hratchian, H. P.; Izmaylov, A. F.; Bloino, J.; Zheng, G.; Sonnenberg, J. L.; Hada, M.; Ehara, M.; Toyota, K.; Fukuda, R.; Hasegawa, J.; Ishida, M.; Nakajima, T.; Honda, Y.; Kitao, O.; Nakai, H.; Vreven, T.; Montgomery, J. A.; Peralta, J. E.; Ogliaro, F.; Bearpark, M.; Heyd, J. J.; Brothers, E.; Kudin, K. N.; Staroverov, V. N.; Kobayashi, R.; Normand, J.; Raghavachari, K.; Rendell, A.; Burant, J. C.; Iyengar, S. S.; Tomasi, J.; Cossi, M.; Rega, N.; Millam, J. M.; Klene, M.; Knox, J. E.; Cross, J. B.; Bakken, V.; Adamo, C.; Jaramillo, J.; Gomperts, R.; Stratmann, R. E.; Yazyev, O.; Austin, A. J.; Cammi, R.; Pomelli, C.; Ochterski, J. W.; Martin, R. L.; Morokuma, K.; Zakrzewski, V. G.; Voth, G. A.; Salvador, P.; Dannenberg, J. J.; Dapprich, S.; Daniels, A. D.; Farkas; Foresman, J. B.; Ortiz, J. V.; Cioslowski, J.; Fox, D. J., Gaussian, Inc.: Wallingford CT, 2013.
21. Dolomanov, O. V.; Bourhis, L. J.; Gildea, R. J.; Howard, J. A. K.; Puschmann, H., *J. Appl. Cryst.* **2009,** *42*, 339-341.
22. Sheldrick, G. M., *Acta Cryst. A* **2015,** *71*, 3-8.
23. Sheldrick, G. M., *Acta Cryst. C* **2015,** *71*, 3-8.
24. Kenning, D. D.; Mitchell, K. A.; Calhoun, T. R.; Funfar, M. R.; Sattler, D. J.; Rasmussen, S. C., *J. Org. Chem.* **2002,** *67*, 9073-9076.
25. Dieguez, H. R.; Lopez, A.; Domingo, V.; Arteaga, J. F.; Dobado, J. A.; Herrador, M. M.; Quilez del Moral, J. F.; Barrero, A. F., *J. Am. Chem. Soc.* **2010,** *132*, 254-259.

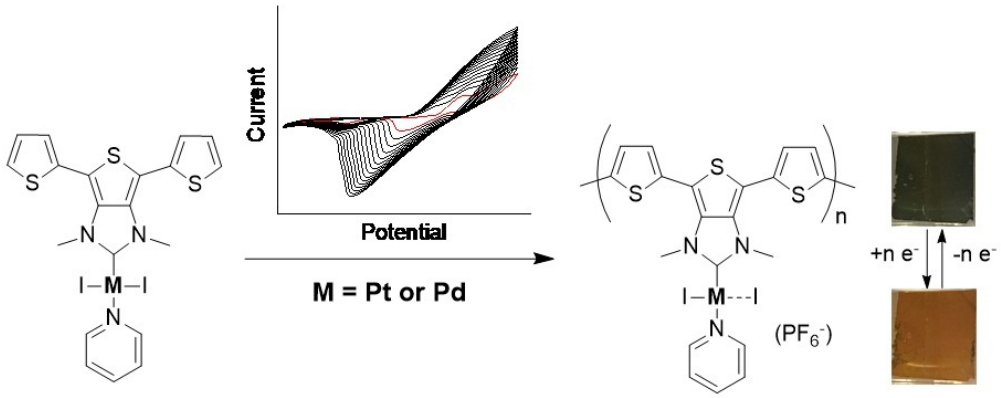

159x68mm (144 x 144 DPI)